

Energetic benefits of elastic spine actuation for a quadrupedal robot

Jeffrey M. Duperret*, Jason L. Pusey†, G. Clark Haynes◇, and D. E. Koditschek*

Abstract—We present preliminary bounding data generated by Canid, a freestanding, power-autonomous, spine-actuated quadrupedal robot. In contrast to other such machines that have recently appeared in the literature or popular media, Canid’s spine motors act in parallel with substantial elastic spine compliance. We explore the energetic consequences of this design in comparison to a pronking gait implemented on XRL, an instance of the stiff-backed, hexapedal RHex design built from electromechanical modules nearly identical to Canid’s. Notwithstanding the advantages of the more mature XRL pronking behavior, Canid bounds in a considerably higher energetic regime but exhibits comparable specific resistance. We show that Canid’s spine contributes to its energetic advantage and that parallel elastic actuation (as opposed to a purely actuated spine) is required for peak performance, which in future work will likely exceed pronking on XRL in specific resistance as well as speed.

I. INTRODUCTION

A. Motivation

After decades of work on rigid body legged platforms [1], robotics researchers have begun to report exciting demonstrations [2] of new [3], and even revolutionary [4] designs for flexible, spine-actuated, quadrupedal runners, with the most impressively novel and promising concepts focused on high performance legs [5]. In contrast, animal tetrapods have a 400 million year history [6] of which only a very little was spent developing “emancipated” therian legs [7], with a long prelude of locomotion generated primarily by high powered “thrusting” of the trunk [8]. In this paper we compare the energetics of locomotion between two running machines that are as similar as we can reasonably devise modulo the central question: what is so good about a high powered, “thrusting” spine?

The design of our new machine, Canid (shown in Fig. 1), detailed in [11], is introduced in [9] along with its stiff-backed conventional alternative XRL (a RHex [12] class machine), as exemplars of the rapid morphological prototyping enabled by an electromechanically conventional and modular “laboratory on legs” kit, which likely explains what we believe to be its claim to first free-standing operation amongst a growing number of flexible spine-actuated quadrupedal machines. Given our commitment to standard commercial off the shelf components, the “high powered

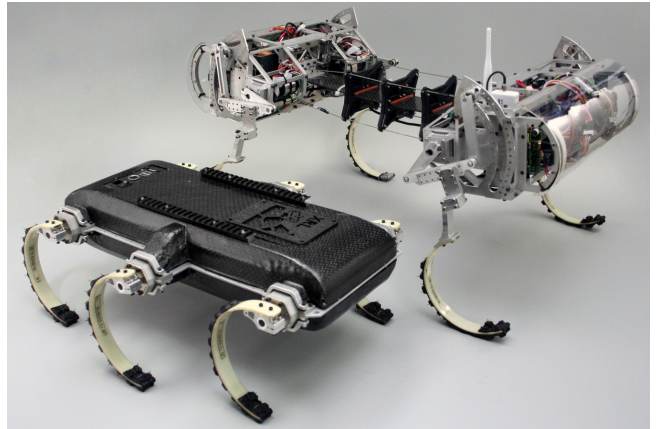


Fig. 1: Canid (top) is built largely from components of XRL (bottom) [9]. Modulo the spine and four-bars, the architecture of these robots is nearly identical as discussed in Section II-A¹.

| Energetic Operating Regime | Canid | Pronking XRL |
|-------------------------------------|-----------------|-----------------|
| Mean Body Energy ² (J) | 59 ± 12 | 26 ± 2 |
| Height-Shifted Mean Body Energy (J) | 39 ± 12 | 20 ± 2 |
| Specific Resistance[10] | 2.13 ± 0.14 | 2.65 ± 0.08 |

TABLE I: Canid operates in an energetic regime nearly double that of XRL pronking (Fig. 3, 4) while exhibiting superior efficiency (Fig. 2), despite being built from nearly identical electromechanical modules and equipped with an identical power budget. The above “height-shifted mean body energy” is equal to mean body energy (measured after XRL achieves steady-state behavior) minus the mass center’s gravitational potential energy at rest so as to not unfairly advantage the taller robot.

thrusting spine” concept necessarily translates into a parallel elastic actuator design, for paramount among the many constraints on autonomous robot performance is that of limited actuator power density. After decades of attention paid to material constituents [13], it seems clear that only a new generation of highly integrated actuation systems — thermoelectromechanical [14], [15] or perhaps thermofluidic [16] — will achieve substantially greater specific power than the 10-100 W/kg range that is presently observed in animals [17] and available (at the lower end of this specific power range) to the robot designer from commercial off the shelf technology [18]. Limited to that conventionally available range, parallel elastic actuation allows a designer’s strong-but-slow motor to transfer energy into a more fungible mechanical energy store which can then release it in a higher force and speed regime programmed to suit the required task. Indeed, many mechatronics researchers have embraced such

* Electrical and Systems Engineering Department, University of Pennsylvania, 200 South 33rd Street, Philadelphia, PA 19104 {jdup,kod}@seas.upenn.edu

† Army Research Laboratory, Aberdeen, MD

◇ NREC, Carnegie Mellon University, Ten 40th St, Pittsburgh, PA 15201 gch@cs.cmu.edu

¹Photographs courtesy of Ryan Knopf.

designs [19], particularly in biologically inspired locomotion applications such as active human prosthetics [20], as well as our setting of highly energetic robotic gaits [5], [21], [22].

B. Contributions

The central contributions of this paper are summarized in Table I. Canid operates in an energetic regime in which the body energy² is on average 40J higher than that of its mass center gravitational potential energy at rest. In contrast, whereas pronking is the most highly energetic sustained gait achieved in RHex class machines [23], XRL’s pronk operates at an average of 20J body energy above that of its mass center gravitational potential energy at rest. Yet Canid’s gait is no less energetically efficient than XRL’s, in fact exhibiting a 20% lower specific resistance (SR) over the course of these trials. Specific resistance values for the robots are derived from Fig. 2 by dividing the weight-normalized output energy by the distance traveled of each robot. Thus, with only 1.5 times its body mass (see Table II), Canid’s bound operates at nearly twice XRL’s pronk energy, with a slightly lower cost of transport, suggesting the beginnings of an answer to the central question just posed.

Although steady-state locomotion is now well advanced across the field [1], robotics has yet to achieve the sort of explosive agility and accompanying rich transient mobility behaviors that truly justify legs; not just running but also leaping, dodging, recovering, etc. Absent super-powered actuation, the energy to fuel such highly dynamic changes must already be available in mechanical form at the time it is needed, thereby enabling the desired rapid changes in body state via limb-recruited application of appropriate ground reaction forces characteristic of the animals. Thus, we believe that platform designs and locomotory styles characterized by high body energy represent the antecedent (if not yet the hallmark) of nimble operation.

The second contribution of the paper is an empirical analysis of Canid’s bound and XRL’s pronk that begins to suggest how the parallel elastic actuated spine confers its energetic benefits. We believe that some aspects of the empirical analysis are new and may be of broader interest. For example the notion of “instantaneous specific resistance” (iSR, see Section III-C.1) — which to the best of our knowledge has not previously been discussed in the literature — has proven quite useful in our growing understanding of how Canid differs from XRL pronking and may be independently useful to other researchers in the field.

C. Organization

In Section II we present and contrast the Canid and XRL platforms as well as their behavioral repertoire. In Section III we describe the details of the comparative study, review the results, and examine the energetic differences between the two robots. In Section IV we discuss the energetic benefits conferred by Canid’s spine in the experiments and argue

²In this paper “body energy” refers to the sum of kinetic and potential energy of the mass center along with the potential energy available in the limb and body elastic compliance.

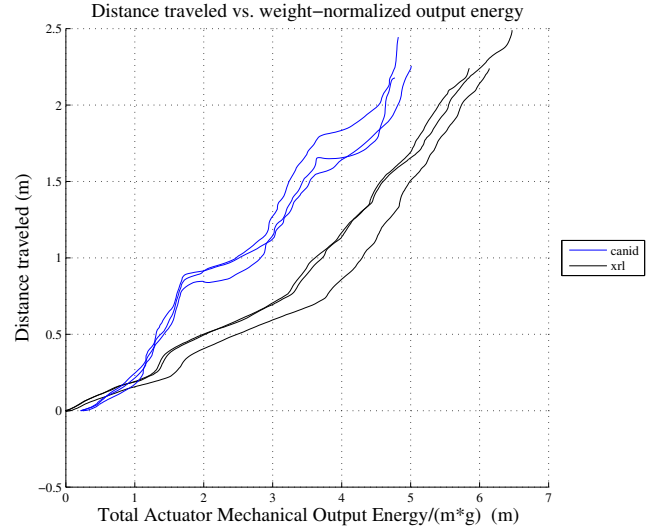


Fig. 2: Center of mass distance traveled vs weight-normalized actuator energy expenditure. The ratio of these is equal to specific resistance, thus Canid’s bound has a lower specific resistance than XRL’s pronk. The slopes of the traces indicate Canid is more efficient than XRL during XRL’s transient acceleration before reaching steady-state (before 0.75m distance traveled), after which both robot’s efficiencies are approximately the same.

that a parallel elastic actuated spine can enable performance superior to that of a purely actuated spine. The paper concludes with a brief summary and speculative remarks about future work.

II. COMPARING A BOUNDING QUADRUPED TO A PRONKING HEXAPOD

A. The Canid and XRL Platforms

The Canid robot is a freestanding, power-autonomous quadruped designed to test hypotheses regarding dynamic bounding using an parallel elastic actuated spine mechanism. Canid was rapidly prototyped using modular components of the XRL hexapod, replacing the two middle legs with a doubly actuated elastic spine mechanism [11], [9]. XRL is a recent member of the RHex family of robots, designed to be a lighter version of its contemporaries without cost to actuator performance [9] — making it both the best equipped of the RHex class to perform dynamic locomotion tasks (and thus act as an adversarial platform with which to compare Canid) and the most similar to Canid as can reasonably be achieved in morphology modulo the spine and four-bar. A brief contrast of Canid and pronking on XRL is shown in Table II and an in-depth summary of both is given in [9].

At a systems level, Canid and XRL have similar architectures. They both use a single PC/104+ computer and are powered by two onboard Thunder Power 10-cell lithium polymer batteries. The batteries are managed by a custom board developed by the University of Pennsylvania’s GRASP lab [24]. Each robot is actuated by 6 very similar motors connected to planetary gearboxes. These motors are all controlled using the same commercial off the shelf AMC motor controller boards that mount to a custom built interface also created within the GRASP lab [24]. Both designs utilize

| | Canid | Pronking XRL |
|---|-------------|--------------|
| Mechanical Design Parameters | | |
| Mass (kg) | 11.3 | 7.3 |
| Body Length (m) | 0.78 | 0.51 |
| Front Hip to Rear Hip Length (m) | 0.39 | 0.41 |
| Maximum Hip Height (m) | 0.288 | 0.152 |
| Electrical Design Parameters and Operating Statistics | | |
| Max Allowed Motor Voltage (V) | 34 | 34 |
| Listed Motor Power (W) | | |
| -Front | 70 | 50 |
| -Middle | 50 | 50 |
| -Rear | 50 | 50 |
| Mean Observed Electrical Power (W) | | |
| -Front (2 motors combined) | 34 ± 52 | 80 ± 78 |
| -Middle (2 motors combined) | 115 ± 98 | 187 ± 153 |
| -Rear (2 motors combined) | 219 ± 205 | 95 ± 93 |
| -Total (6 motors combined) | 368 ± 271 | 362 ± 233 |
| Robot Body Operating Statistics | | |
| Mean Stride Length (m) | 0.82 ± 0.09 | 0.53 ± 0.06 |
| Mean Stride Frequency (Hz) | 1.31 ± 0.11 | 3.50 ± 0.24 |
| Mean Duty Factor | 0.55 ± 0.04 | 0.23 ± 0.04 |
| Mean Steady-State Forward Vel. (m/s) | 1.38 ± 0.19 | 1.86 ± 0.13 |
| (body-lengths/sec) | 1.97 ± 0.27 | 3.65 ± 0.26 |
| Maximum Forward Velocity (m/s) | 2.18 | 2.11 |
| (body-lengths/sec) | 2.79 | 4.14 |

TABLE II: Parameters and statistics comparing Canid to pronking on XRL. The observed stride length, stride frequency, duty factor, and motor power statistics for XRL are calculated after the robot has achieved steady-state behavior. The “steady-state” velocity for Canid is computed from ensemble data restricted to aerial phase (see Fig. 6).

the same elastic C-shaped legs pioneered for RHex [25], [26] to refine contact kinematics with the substrate, dampen ground impacts and provide a means of mechanical energy storage. While the robots do not have the same body mass (see Table II), we can account for this by using specific resistance (SR) as our metric for efficiency.

Canid’s most significant divergence from the RHex family is the introduction of its flexible spine: a carbon fiber flat plate antagonistically actuated by 2 sets of cables that allow it to pitch up and down (driven, in turn, by 2 appropriately antagonistic motors). This design was introduced in [9] and is discussed at length in [11]. The carbon fiber plate acts as a leaf spring that stores and releases energy throughout the gait. The plate is rigidly attached to 3 vertebrae that the actuating cables are threaded through to allow for control of the spine’s curvature.

Canid’s second key design divergence from XRL (and the RHex family in general) arises from the presence of a four-bar mechanism inspired by the RiSE robot series [27] that connects each leg motor to a C-leg. The four-bar mechanism modifies the leg’s toe-path, increases Canid’s height-to-length ratio, and provides a variable transmission throughout the stride. The variable gearing is intended to supply low speed and high torque during ground contact, followed by high speed and low torque during aerial recirculation.

B. Comparing Gait Behaviors

Although we presently lack a rigorous understanding of how to compare gaits for purposes of energetic insight,

pronking seems to be the most appropriate candidate for early comparison between the RHex and Canid designs. RHex pioneered locomotory energy management behavior as a generalist [28]. Originally inspired by arthropod (hexapedal) trotting [29], it is capable of (quadrupedal) bounding [30], as well as pronking [23], and more recently leaping [31] (although not in a sustained fashion suitable for comparison) — of which only the latter two modes represent the highest body-energetic operation the design seems capable of achieving without careful optimization. RHex’s quadrupedal bounding operates in a lower energetic regime than pronking (7.5 kg traveling at 1.5 m/s with 35% aerial phase representing body energy of around 10J) but this economy does not seem to confer superior efficiency (a SR of 2.08-4 depending upon speed)[30], and in any case, it is not clear how to compare directly gaits using 6 actuators against those using just 4³. Its “native” (alternating tripod) trot traverses level ground at well under half that of Canid’s SR, but such gaits typically operate in a very low energetic regime (speeds at roughly a body length per second, with associated body energies of less than 10J) [32]. Highly optimized alternating tripod gaits [32] with body energy exceeding 25J (7.5 kg traveling at 2.7 m/s with 35% aerial phase) match the energetics of XRL’s pronking steady-state operation we report here (see Fig. 4) with dramatically lower SR (0.84) but they entail detailed insights into the nature of this well studied gait [33]. In contrast, neither RHex pronking nor flexible spine bounding are yet well enough understood to permit comparably optimized performance.

The distinctly different nature and lineage of these two designs confer upon XRL two important advantages that *a priori* lend these experiments an adversarial aspect for Canid. Most importantly, XRL represents the third generation upgrade and re-design [9] of a decade-old concept [12] that has already proved successful at highly dynamic behaviors [31]. Second, mature insight into the SLIP template [34], [35] and a growing understanding of its RHex pronking anchor [36], [37], gives us an open-loop stable [38], [39] attractor basin toward which we guide XRL’s state while pronking. In contrast locomotion science has not yet settled on even a candidate template for bounding, leaving Canid deficient of a clear and rational anchoring strategy as a target for our open-loop control to achieve.

III. EXPERIMENTS

A. Setup and Results

The comparative study consisted of 3 successful runs of Canid bounding and 3 successful runs of XRL pronking, with both robots operating under body-open-loop control (i.e., all motors are excited by local PD controllers forced by pre-planned, open-loop feed-forward reference trajectories). Each Canid run contained 3 strides and each XRL run contained 4-5 strides, which were recorded under a Vicon motion capture system⁴ for measurement of the robot kinematics⁵.

³For this same reason we did not lock Canid’s spine as a comparison because we would also be using 4 actuators.

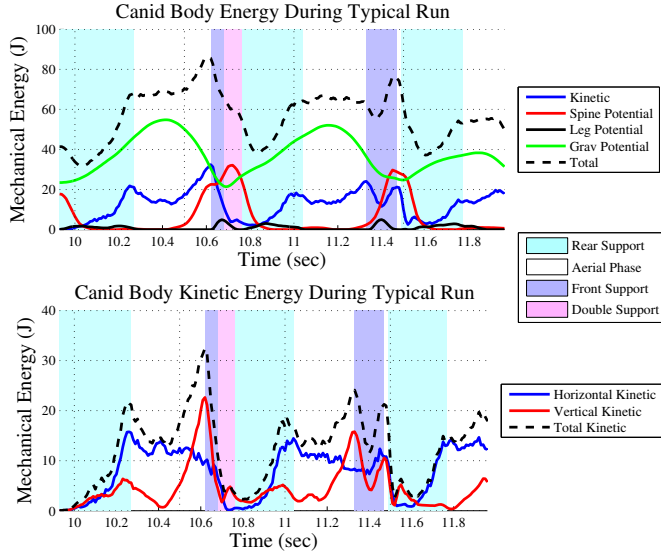


Fig. 3: Body energy for Canid during a typical run. The plot illustrates that Canid stores a mean maximum of 31J in its spine during each stride after its first bound (which is a sizable 53% of the total mean body energy of 59J), as well as approximately double the leg elastic energy achieved by XRL pronking (calculated in [11]). Canid does not achieve a steady-state condition; its total mechanical body energy fluctuates widely around an average of 59J. In particular, nearly all horizontal kinetic energy is lost between strides due to open-loop inefficiencies as discussed in Section III-B.2. Due to these inefficiencies, it is likely that at present only a small fraction of the elastic energy stored in the spine is being put to useful work in the subsequent leap (largely, we surmise, through some transfer to the rear leg springs during front lift off).

The per-stride statistics given in this paper contain only XRL’s steady-state behavior and the first 2 Canid strides of each run — since Canid uses the 3rd landing to decelerate and safely come to rest, and thus the 3rd stride doesn’t represent fully operational bounding behavior.

B. Typical Canid and Pronking XRL Strides

1) *A Typical Canid Stride*: Canid’s current intended gait dynamics can be described as a hybrid dynamical system in which there are 4 possible phases: rear-support, aerial phase, front-support, and double-support. An in-depth breakdown of a typical Canid stride during the experiments is given in [11], and a brief description of each hybrid phase is given as follows.

(a) *Rear-Support*: Canid typically starts crouched and flexing its spine — its front legs having just lifted off from double-support, leaving only the rear legs in contact with the ground. During the course of the stance, the rear legs push off and the spine both launches the front mass and imposes inertial forces upon the rear legs. The spine accomplishes this through the parallel release of stored elastic spine energy and

⁴<http://www.vicon.com>

⁵Using three strides was chosen because it fits easily within the space constraints imposed by our Vicon facility, is long enough to gather the data we need, and can be readily accomplished in a few days of gait tuning following small changes to the machine. Since Canid does not accelerate significantly between strides due to the uncoordinated (open-loop) rear touchdowns described in Section III-B.2, we are convinced that more strides per run would yield quantitative results very similar to the current setup.

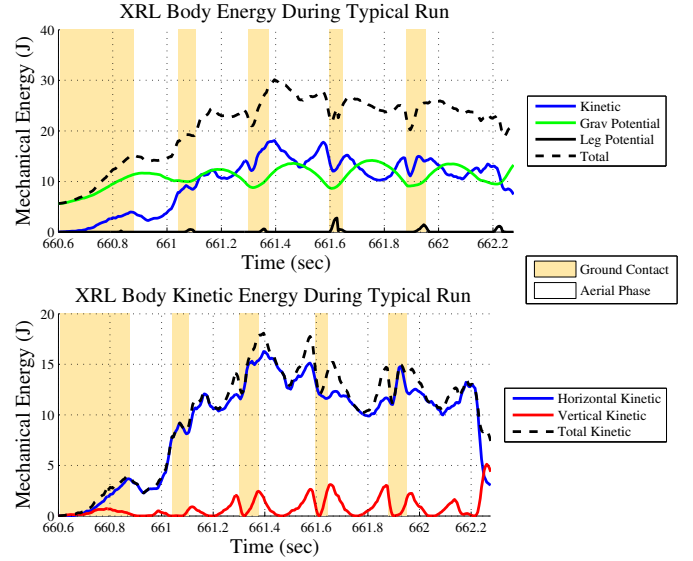


Fig. 4: Body energy for XRL during a typical run. The plot illustrates that XRL’s pronk operates in steady-state at a mechanical body energy of approximately 25J. There is relatively little energetic contribution made by the leg elastic elements, less than half that achieved in Canid.

actuation via the top spine cables. Details of the spine and its empirical characterization (as well as that of the legs) are given in [11].

(b) *Aerial Phase*: Canid’s total body energy is relatively constant, save for an increase near the end due to work on the spine by the motors. The front and rear legs are recirculating during this interval.

(c) *Front-Support*: Vertical kinetic energy immediately begins to decrease upon front leg touchdown as Canid converts it into spring potential energy in the spine and legs. By the end of spine compression, Canid has stored a very significant quantity of potential energy in the spine — almost 50% of its aerial phase apex body energy — as illustrated in Fig. 3.

(d) *Double-Support*: Both legs are often but not always in brief simultaneous ground contact: this was seen in 4 out of the 6 measured strides, and its varied appearance is attributed to open-loop disturbances described in Section III-B.2. Work in progress aims to determine what advantages (if any) a Canid double-support strategy has over the more rarely observed alternative (short) aerial phase.

2) *Canid’s Uncoordinated Open-Loop Gait*: Wasteful loss of forward kinetic energy occurs during each new rear stance, as illustrated in Fig. 3(b) and established in Fig. 6. In [11] we show that much of this energy is consumed in uncontrolled roll perturbations at the beginning of each new rear leg stance phase consequent upon uncoordinated touchdowns. This waste manifests itself in Fig. 6 as contributing an explosively bad iSR measure and hence represents the chief culprit in Canid’s inability to sustain within-stride efficiency since there is little loss of fore-aft energy (and correspondingly low iSR) during the aerial and front leg support phases. Due to these inefficiencies, only a small fraction of energy stored in the elastic spine is likely being put to useful work in the

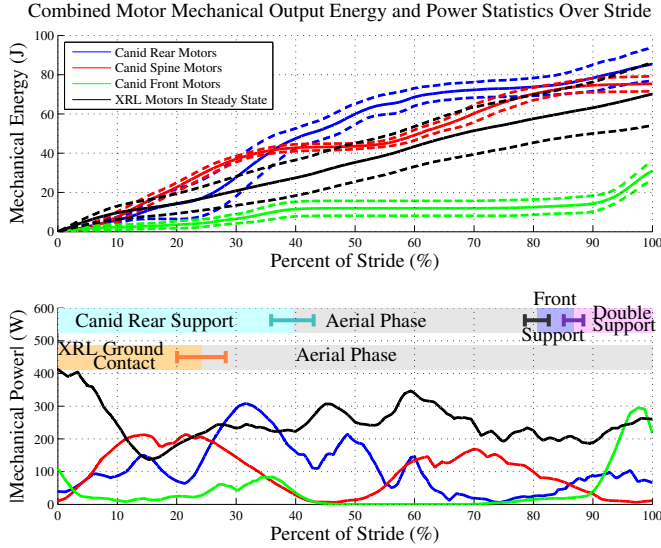


Fig. 5: Comparison between the total motor mechanical output cost of Canid and pronking XRL. Solid lines correspond to mean values while dashed lines and error bars correspond to one standard deviation from the mean. On average Canid spends 36% (70J) of its total output energy of 192J per stride during aerial recirculation, while XRL spends 76% (53J) of its total output energy of 70J during aerial recirculation. While over the course of a stride both robots do approximately the same work to recirculate their legs, Canid's leg motors use less power due to the lower stride frequency (see Table II), giving it the iSR advantage over XRL during flight as measured in Fig. 6 and discussed in Section III-C.2. Only steady-state XRL pronking behavior is shown.

subsequent leap (largely, we surmise, through some transfer to the rear leg springs during front lift off).

3) *A Typical Steady-State Pronking XRL Stride*: A stride for XRL's pronk begins when the legs contact the ground (leg touchdown). As shown in Fig. 4, the energy exchange on landing stores some potential energy in the legs but typically only about half that of Canid. All the legs push off the ground in unison to propel XRL into flight. Upon liftoff, XRL recirculates its motors in anticipation of the subsequent ground contact.

C. Energetic Comparison

To facilitate energetic comparison between similar mechanical conditions, the stride of each robot is partitioned into an aerial interval and a leg-ground contact interval. To aid in this analysis we first introduce the concept of instantaneous specific resistance.

1) *Instantaneous Specific Resistance*: We define instantaneous specific resistance (iSR) as:

$$\frac{P}{mg\dot{x}}$$

where P is the instantaneous motor mechanical output power, m is the robot's mass, g is acceleration due to gravity,

⁶To smooth out high frequency noise, in Fig. 6(a) we plot moving average instantaneous specific resistance, or $\bar{P}/mg\bar{\dot{x}}$, where \bar{P} and $\bar{\dot{x}}$ are the moving average of P and \dot{x} , respectively. The moving average window was chosen to have length 5 and the data is given at 200Hz. The reader can verify that as the moving average window gets larger and larger it will approach the standard $\Delta E/mg\Delta x$ definition of specific resistance.

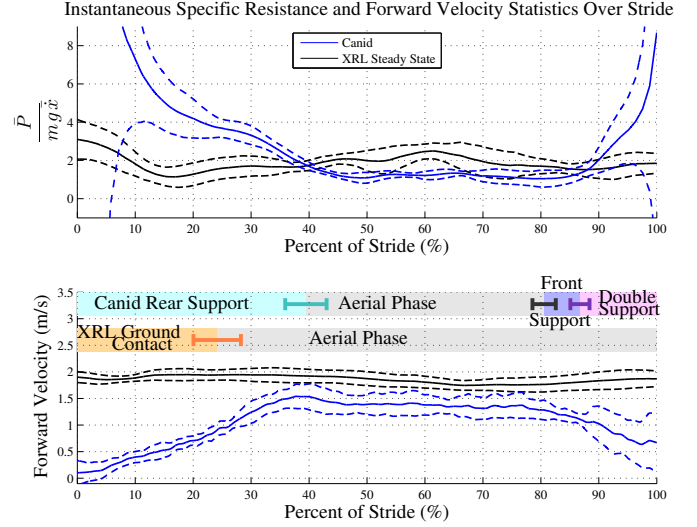


Fig. 6: iSR and velocity statistics over the course of a stride. Solid lines correspond to mean values while dashed lines and error bars correspond to one standard deviation from the mean. Canid's present open-loop controller loses the majority of its fore-aft velocity accumulated over the prior stride when the rear legs touch down, hence at near zero velocity it incurs huge instantaneous specific resistance at the beginning of each stride. During flight, Canid's iSR is less than that of XRL's, indicating that Canid's recirculation mechanics are more efficient. Only steady-state XRL pronking behavior is shown. See Section III-C.1 for iSR definition⁶.

and \dot{x} is the robot's forward velocity. The iSR measure is used in Fig. 6⁶ to evaluate locomotion efficiency at a particular stride phase.

It is worth mentioning that iSR differs from the conventional notion of SR in ways that can give conflicting results. If a moving robot suddenly comes to rest with little energy expenditure then its SR will not change dramatically, however the iSR will increase without bound due to the denominator of the quotient being zero. This means that when Canid loses its forward velocity on each bound due to open-loop inefficiency, the iSR blows up while the SR only sees a moderate increase as contrasted in Figures 6 and 2.

2) *Energetic Comparison of Aerial Interval*: The traces of each machine in Fig. 6(a) show that Canid has a lower iSR (and hence a higher efficiency) than XRL's pronk only during the aerial phase, an observation echoed by the slopes of the traces in Fig. 2. The aerial phase incurs a high energetic cost for both robots as shown in Fig. 5(a) during which Canid expends 36% of its stride energy and XRL expends 76% of its stride energy, making this interval significant in the energetic efficiencies of both machines.

The main energetic costs in aerial phase are leg recirculation and (for Canid) loading up the spine. Fig. 5(a) shows that Canid's mean recirculation cost per leg per stride is higher than XRL's (12.6 J vs. 8.9 J, respectively), and thus Canid's aerial energetic advantage over XRL cannot be explained by favorable recirculation gearing of its four-bars. Motor measurements presented in [11] confirm that neither machine is disadvantaged by its leg actuator torque limits which are never reached in either behavior. Fig. 5(b) reveals that

Canid's higher recirculation efficiency is consequent upon its longer aerial phase affording more time to work upon the spine and recirculate the legs with less power. Canid and XRL expend nearly the same total recirculation energy per stride. Even when we antagonistically label Canid's spine motor energy during flight as part of "recirculation," Canid spends on average of 70J vs. XRL's 53J (see Fig. 5(a)), but because XRL's stride frequency is more than twice that of Canid's (see Table II), XRL expends 101% more recirculation energy in a given time interval than Canid would (including spine energy).

3) *Energetic Comparison of Ground Contact Interval:* Canid's ground contact interval is currently very inefficient (see Figures 2, 5) as discussed in Section III-B.2. Nevertheless, Canid's first bounds average better than a tripling of XRL's pronking distance traveled relative to the same (mass normalized) mechanical actuator output energy. Likely causes of Canid's more efficient initial acceleration include its doubled recruitment of elastic leg energy (see Figures 3 and 4) through leg forces generated by the four-bars and in reaction to the rapid extension of the spine.

IV. DISCUSSION

Over the course of a typical stride, Canid's actuators output a mean total mechanical energy more than 2.7 times that expended by XRL's in work on their respective mass centers according to Fig. 5(a). However the stride length statistics of Table II show that Canid uses this mechanical energy to drive its mass center on average almost 1.6 times farther than XRL per stride. Hence XRL's mass-normalized cost of transport in steady-state is roughly comparable to Canid's (see Fig. 2), despite Canid almost doubling the energetic regime of XRL pronking as depicted in Figures 3 and 4.

The iSR trajectories in Fig. 6 show that Canid's efficiency would likely exceed pronking XRL's throughout much of its (considerably longer) stride, had we introduced feedback to better control the (presently) highly disordered interval of its rear legs' ground contact phase. Ultimately, even in this early study, because open-loop Canid accelerates more efficiently from rest than open-loop pronking XRL can (compare the slopes of the two machines' mass center position during the initial 3/4 meter travel in Fig. 2) Canid's overall mass-normalized cost of transport is 20% lower.

As reviewed in Section II-A, Canid incorporates two design innovations relative to XRL: its longer legs (with linkages) and its spine. Longer legs confer longer stride, and while we have observed in Section III-C.2 that Canid's leg

recirculation cost is 1.42 times greater than XRL's pronk per stride, it must be the case that the variable gearing of the linkages plays some significant role in attenuating the effects of the roughly quadrupled inertial load (owing to doubled leg length)⁷. A detailed accounting of the relative contributions to energetic efficiency of these two different design innovations is not possible given our present instrumentation and modeling since the kinematics of ground contact by the shaped, elastic legs of both machines is complex (and different), and the spine's relatively small range of kinematic motion of ± 6 cm belies its significant dynamical influence on stride length (whose exploration lies beyond the scope of the present paper). For purposes of this paper, focused as it is on the spine, it suffices to detail the direct manifestation of the spine's energetic benefit.

A. Role of Canid's Spine

In Section III-B.1.c we observed that the spine collects nearly 50% of the body's aerial-apex energy through its compression (via motor actuation and the inertial force of the falling rear) during front leg ground contact. A more decisive test of its value is whether it can also add energy to the body during a stride's initial leap. We first show that the spine indeed adds energy to the body during leaping, and then examine how the collected spine potential energy might be usefully harvested by a more coordinated (closed-loop) future gait.

1) *Spine Energetic Contribution:* Fig. 5 shows that the rear motors output on average 47J through their output shafts during rear stance phase (roughly the 0-40% phase interval). We show in [11] that motor gearbox mechanical efficiency is 70%, hence less than 33J of body energy during a leap can have been contributed by these actuators. But Fig. 3 shows that after excluding the initially stored spine spring energy, Canid's total body energy increases by at least 40J during the two leaps depicted (all of which occurs in rear stance phase). The more complete data set in [11] shows that this is true of the first and second leaps for all runs measured. It is clear, then, that Canid's "powerful thrusting spine" is contributing at least roughly 20% of the total mechanical energy its body accumulates during a leap (and certainly more⁸). While more analysis and redesign will likely result in considerably greater efficiency, it is already clear that the parallel elastic actuated spine is directly contributing to Canid's mechanical body energy during a leap.

2) *Spine Energy Collection and Release:* Having shown just above that the spine is responsible for at least 1/5 of Canid's total body energy accumulated during a leap, we must now establish where that energy goes during the course of a complete stride. Whereas thermal limitations preclude our pre-loading Canid's spine with more than 18J prior to a run, Fig. 3 illustrates how another 100% more energy than

⁷Due to toe-stubbing in Canid's rear legs on liftoff documented in [11], the rear legs reverse direction at the beginning of aerial recirculation to pass back through a portion of the high-torque, low-speed angular position interval of the four-bar, before again reversing directions (and again poising through this high-torque, low-speed interval) before reaching the high-speed, low torque regime of the four-bar that is intended for leg recirculation as described in Section II-A. Thus we expect that without toe-stubbing Canid will have a lower energetic cost of leg recirculation, because Canid will get the full benefit of its four-bars. However some form of toe stubbing may be required for stable running [23], [31].

⁸Work remains to characterize the mechanical efficiencies of the leg, spine, and four-bar mechanisms. Without such characterization it is difficult to calculate what percentage of Canid's body energy came from the spine, but given that such mechanisms must be less than 100% efficient we expect the spine contribution to be significantly greater than 1/5.

this 18J is typically collected in the spine after the first leap from a combination of kinetic, gravitational potential, and actuator-applied energy.

We have already observed (Section III-B.1.c) that the energy accumulated in the spine at a stride's end is substantial, but is unfortunately not presently reinvested toward the energetic cost of the next leap due to the uncoordinated rear touchdowns (Section III-B.2). In contrast, the initial spine spring energy stored by the actuators prior to the first leap (e.g., the red trace of Fig. 3 starts at 18J stored) accelerates Canid from rest considerably more efficiently than XRL as seen in the initial traces of Fig. 2. Hence, we are encouraged to believe that closed-loop coordination now under development will result in far more efficient Canid gaits at considerably greater steady-state speed.

B. Parallel Elastic Actuated Spine vs. Purely Actuated Spine

Having shown that Canid's powerful "thrusting" spine is indeed contributing useful work to the robot's mechanical body energy and thereby to its favorable efficiency relative to XRL's pronk, we are now interested in exploring the benefits of its specific parallel elastic actuated design over a purely actuated design.

Observe from the red trace of Fig. 3(a) that the potential energy stored in Canid's spine releases very quickly during the period when the rear legs are in stance. In particular, note that there is release of more than 30J during a period of time just over 100ms: more detailed data presented in [11] shows that these releases occur with greater than 210W peak power. At the same time, Fig. 5 suggests (and the data in [11] corroborate) that the individual motor responsible for flexing the spine during this liftoff phase is working at more than 85W. Thus, even in the present very wasteful and constrained regime of operation, Canid's spine outputs more than 295W peak power during this phase of operation. For comparison, all 6 of XRL's motors combined output a maximum power of 414W in an average steady-state pronking stride as shown in Fig. 5(b), only 40% above the output of Canid's spine alone during its liftoff phase. Thus on Canid the parallel elastic actuated spine design confers the benefit of increased maximum power output that wouldn't be available in a similar but purely actuated spine design.

V. CONCLUSION

We have presented a detailed empirical energetic analysis of Canid's preliminary (unsteady, open-loop) bounding — to the best of our knowledge, the first time operational data has been presented for a free-standing, power-autonomous quadruped with an actuated flexible spine. Given the very early character of this design we feel that Canid shows remarkable energetic promise since it performs quite competitively as an early prototype in an adversarial comparison to the much more mature platform XRL operating in a (somewhat) better understood behavioral regime. Namely, Canid operates at an energy level nearly twice that of XRL pronking (39J vs 20J of body energy beyond gravitational potential at rest). Indeed, as an early manifestation of the

potential value of such highly energetic operation, Canid accelerates much more efficiently from rest than XRL which allows comparable energetic performance despite Canid's uncoordinated loss of forward velocity between strides. Quantitatively, including transient periods of acceleration, Canid already exhibits slightly better specific resistance than XRL (2.13 vs. 2.65, respectively). A close examination of the data reveals that Canid gains an energetic advantage over XRL by using less power during recirculation than XRL due its longer stride length and lower stride frequency. The data also reveals that the spine does not merely collect apex energy as the body falls back down, but actually contributes body energy during the following leap. Finally we observe that the parallel elastic actuation plays a key role: Canid could not achieve its present rate of work without the boosted speed-force profile conferred by the elastic spine.

In sum, we tentatively conclude that a powerful "thrusting" spine is energetically valuable because it allows a running body to accumulate and maintain a large store of mechanical energy on hand (at the ready for when a very rapid change of state is required) without undue losses along the way. We expect that work now in progress on Canid will achieve substantial performance gains through closed-loop control. While this rapidly prototyped, electromechanically modular machine is unlikely to set dramatic new speed records, we trust that its higher performance regimes will promote sharper new hypotheses concerning bounding in animals and robots by facilitating systematic comparison to established, better understood, and relatively poorer performing prior designs.

ACKNOWLEDGEMENTS

The authors thank Ryan Knopf for contributing to the design and construction of Canid, Aaron Johnson for both paper editing and contributing to the XRL pronking behavior development, and Martin Buehler for discussions about RHex pronking.

This work is supported by the National Science Foundation Graduate Research Fellowship under Grant No. DGE-0822 and by the Army Research Laboratory under Cooperative Agreement Number W911NF-10-2-0016.

REFERENCES

- [1] X. Zhou and S. Bi, "A survey of bio-inspired compliant legged robot designs," *Bioinspiration & biomimetics*, vol. 7, no. 4, p. 041001, 2012.
- [2] "Boston dynamics," <http://www.bostondynamics.com>.
- [3] V. Chernyak, T. Flynn, J. O'Rourke, J. Morgan, A. Zalutsky, S. Chernova, S. S. Nestinger, and T. Padir, "The design and realization of a high mobility biomimetic quadrupedal robot," in *Proceedings of 2012 8th IEEE/ASME International Conference on Mechatronic and Embedded Systems and Applications, MESA 2012*, 2012, pp. 93–98.
- [4] G. A. Folkertsma, S. Kim, and S. Stramigioli, "Parallel stiffness in a bounding quadruped with flexible spine," in *IEEE International Conference on Intelligent Robots and Systems*, 2012, pp. 2210–2215.
- [5] S. Seok, A. Wang, D. Otten, and S. Kim, "Actuator design for high force proprioceptive control in fast legged locomotion," in *IEEE International Conference on Intelligent Robots and Systems*, 2012, pp. 1970–1975.
- [6] R. A. Raff, *The Shape of Life: Genes, Development, and the Evolution of Animal Form*. University of Chicago Press Chicago, 1996.

- [7] M. S. Fischer, N. Schilling, M. Schmidt, D. Haarhaus, and H. Witte, "Basic limb kinematics of small therian mammals," *Journal of Experimental Biology*, vol. 205, no. 9, pp. 1315–1338, 2002.
- [8] M. S. Fischer and H. Witte, "Legs evolved only at the end!" *Philosophical Transactions of the Royal Society A: Mathematical, Physical and Engineering Sciences*, vol. 365, no. 1850, pp. 185–198, 2007.
- [9] G. C. Haynes, J. Pusey, R. Knopf, A. M. Johnson, and D. E. Koditschek, "Laboratory on legs: an architecture for adjustable morphology with legged robots," in *Unmanned Systems Technology XIV*, R. E. Karlsen, D. W. Gage, C. M. Shoemaker, and G. R. Gerhart, Eds., vol. 8387, no. 1. SPIE, 2012, p. 83870W.
- [10] T. Von Karman and G. Gabrielli, "What price speed? specific power required for propulsion of vehicles," *Mechanical Engineering*, vol. 72, pp. 775–781, 1950.
- [11] J. L. Pusey, J. M. Duperret, G. C. Haynes, and D. E. Koditschek, "Leaping experiments with a power-autonomous, compliant-spined quadruped," in *Unmanned Systems Technology XV*. SPIE, 2013, to Appear. [Online]. Available: <http://kodlab.seas.upenn.edu/Jeff/SPIE2013>
- [12] U. Saranli, M. Buehler, and D. E. Koditschek, "Rhex: A simple and highly mobile hexapod robot," *International Journal of Robotics Research*, vol. 20, no. 7, pp. 616–631, 2001.
- [13] I. W. Hunter, J. M. Hollerbach, and J. Ballantyne, "A comparative analysis of actuator technologies for robotics," *Robotics Review*, vol. 2, pp. 299–342, 1992.
- [14] B. P. Ruddy and I. W. Hunter, "Design and optimization strategies for muscle-like direct-drive linear permanent-magnet motors," *International Journal of Robotics Research*, vol. 30, no. 7, pp. 834–845, 2011.
- [15] J. Urata, Y. Nakanishi, K. Okada, and M. Inaba, "Design of high torque and high speed leg module for high power humanoid," in *IEEE/RSJ 2010 International Conference on Intelligent Robots and Systems, IROS 2010 - Conference Proceedings*, 2010, pp. 4497–4502.
- [16] D. Dunn-Rankin, E. M. Leal, and D. C. Walther, "Personal power systems," *Progress in Energy and Combustion Science*, vol. 31, no. 5, pp. 422–465, 2005.
- [17] K. Meijer, Y. Bar-Cohen, and R. Full, "Biological inspiration for musclelike actuators of robots," in *Biologically Inspired Intelligent Robots*, pp. 25–41, 2003.
- [18] A. De, G. Lynch, A. Johnson, and D. Koditschek, "Motor sizing for legged robots using dynamic task specification," in *2011 IEEE Conference on Technologies for Practical Robot Applications, TePRA 2011*, Boston, MA, USA, April 2011, pp. 64–69.
- [19] R. Ham, T. Sugar, B. Vanderborght, K. Hollander, and D. Lefeber, "Compliant actuator designs," *Robotics & Automation Magazine, IEEE*, vol. 16, no. 3, pp. 81–94, 2009.
- [20] S. K. Au, J. Weber, and H. Herr, "Powered ankle-foot prosthesis improves walking metabolic economy," *Robotics, IEEE Transactions on*, vol. 25, no. 1, pp. 51–66, 2009.
- [21] G. A. Lynch, J. E. Clark, P. Lin, and D. E. Koditschek, "A bioinspired dynamical vertical climbing robot," *International Journal of Robotics Research*, vol. 31, no. 8, pp. 974–996, 2012.
- [22] D. F. B. Haeufle, M. D. Taylor, S. Schmitt, and H. Geyer, "A clutched parallel elastic actuator concept: Towards energy efficient powered legs in prosthetics and robotics," in *2012 4th IEEE RAS EMBS International Conference on Biomedical Robotics and Biomechatronics (BioRob)*, June 2012, pp. 1614–1619.
- [23] D. McMordie and Buehler, "Towards pronking with a hexapod robot," in *Proc. 4th Intl. Conf. on Climbing and Walking Robots*. Storming Media, 2001, pp. 659–666.
- [24] K. C. Galloway, G. C. Haynes, B. D. Ilhan, A. M. Johnson, R. Knopf, G. Lynch, B. Plotnick, M. White, and D. E. Koditschek, "X-rhex: A highly mobile hexapedal robot for sensorimotor tasks," University of Pennsylvania, Tech. Rep., 2010.
- [25] E. Z. Moore, D. Campbell, F. Grimminger, and M. Buehler, "Reliable stair climbing in the simple hexapod 'rhex'," in *Proceedings - IEEE International Conference on Robotics and Automation*, vol. 3, 2002, pp. 2222–2227.
- [26] E. Z. Moore, "Leg design and stair climbing control for the rhex robotic hexapod," Ph.D. dissertation, McGill University, 2002.
- [27] M. J. Spenko, J. A. Saunders, G. C. Haynes, M. R. Cutkosky, A. A. Rizzi, R. J. Full, and D. E. Koditschek, "Biologically inspired climbing with a hexapedal robot," *Journal of Field Robotics*, vol. 25, no. 4-5, pp. 223–242, 2008.
- [28] U. Saranli, M. Buehler, and D. E. Koditschek, "Rhex: A simple and highly mobile hexapod robot," *International Journal of Robotics Research*, vol. 20, no. 7, pp. 616–631, 2001.
- [29] R. Altendorfer, N. Moore, H. Komsuoglu, M. Buehler, H. B. Brown Jr., D. McMordie, U. Saranli, R. Full, and D. E. Koditschek, "Rhex: A biologically inspired hexapod runner," *Autonomous Robots*, vol. 11, no. 3, pp. 207–213, 2001.
- [30] D. Campbell and M. Buehler, "Preliminary bounding experiments in a dynamic hexapod," *Experimental Robotics VIII*, pp. 612–621, 2003.
- [31] A. M. Johnson and D. E. Koditschek, "Toward a vocabulary of legged leaping," in *Intl. Conference on Robotics and Automation*, 2013, to Appear. [Online]. Available: <http://kodlab.seas.upenn.edu/Aaron/ICRA2013>
- [32] J. D. Weingarten, G. A. D. Lopes, M. Buehler, R. E. Groff, and D. E. Koditschek, "Automated gait adaptation for legged robots," in *Proceedings - IEEE International Conference on Robotics and Automation*, vol. 2004, 2004, pp. 2153–2158.
- [33] D. E. Koditschek, R. J. Full, and M. Buehler, "Mechanical aspects of legged locomotion control," *Arthropod Structure and Development*, vol. 33, no. 3, pp. 251–272, 2004.
- [34] R. Full and D. Koditschek, "Templates and anchors: Neuromechanical hypotheses of legged locomotion on land," in *The Journal of Experimental Biology*, vol. 202, 1999, pp. 3325–3332.
- [35] P. Holmes, R. J. Full, D. Koditschek, and J. Guckenheimer, "The dynamics of legged locomotion: Models, analyses, and challenges," *SIAM Review*, vol. 48, no. 2, pp. 207–304, 2006.
- [36] H. Komsuoglu, D. McMordie, U. Saranli, N. Moore, M. Buehler, and D. E. Koditschek, "Proprioception based behavioral advances in a hexapod robot," in *Proceedings - IEEE International Conference on Robotics and Automation*, vol. 4, 2001, pp. 3650–3655.
- [37] M. M. Ankarali and U. Saranli, "Control of underactuated planar pronking through an embedded spring-mass hopper template," *Autonomous Robots*, vol. 30, no. 2, pp. 217–231, 2011.
- [38] R. M. Ghigliazza, R. Altendorfer, P. Holmes, and D. Koditschek, "A simply stabilized running model," *SIAM Journal on Applied Dynamical Systems*, vol. 2, no. 2, pp. 187–218, 2003.
- [39] A. Seyfarth, H. Geyer, M. Günther, and R. Blickhan, "A movement criterion for running," *Journal of biomechanics*, vol. 35, no. 5, pp. 649–655, 2002.